The Arabidopsis nucleoporins 98A/B are essential for NLP7 nuclear accumulation in response to nitrate

Zsolt Kelemen[1,#] , Garry Duville[1,2,#], Virginie Bréhaut[1], and Anne Krapp[1]*

[1] Université Paris-Saclay, INRAE, AgroParisTech, Institut Jean-Pierre Bourgin for Plant Sciences (IJPB), 78000, Versailles, France

[2] University of Paris-Sud, Université Paris-Saclay, 91405 Orsay, France

[#] These authors have equally contributed.

[*]Correspondence should be addressed to Anne Krapp. e-mail: anne.krapp@inrae.fr

Short title: Loss of NUP98A/B affects NLP7 activity

One-sentence summary: The Arabidopsis nucleoporins 98A/B enable acclimation of Arabidopsis to N status by gating the nucleocytoplasmic trafficking of the nitrate sensor NLP transcription factors.

The authors responsible for the distribution of materials integral to the findings presented in this article, in accordance with the policy described in the Instructions for Authors, are: Zsolt Kelemen (zsolt.kelemen@inrae.fr) and Anne Krapp (anne.krapp@inrae.fr).

Abstract

The nuclear compartment is an essential evolutionary gain in eukaryotes. Stimulus-induced nuclear accumulation of transcription factors allows rapid and reversible regulation of gene expression. Nitrate-regulated nuclear accumulation of the master transcriptional regulator NLP7, a member of the RWP-RK family of transcription factors, triggers a major gene expression cascade. Whether and how this process is regulated at the level of the nuclear pore remains elusive. Here we show that the mobile nucleoporin NUP98A and its close homolog NUP98B interact with NLP7 in the nucleus and that the nitrate-triggered nuclear accumulation of NLP7 is impaired in their absence. We also showed that the simultaneous loss of NLP7 and NUP98A strongly and specifically alters the expression of nitrate-regulated genes and drastically reduces plant growth. Our results indicate that plant NUP98 acts on nitrate use by plants through its interaction with the top-tier NLP7 transcription factor.

Introduction

Nucleoporins (NUPs) are fundamental components of all eukaryotic cells. They are constituents of the nuclear pore complexes (NPCs), which are extremely large protein complexes embedded in the nuclear envelope and consist of over 1,000 copies of ～30 individual NUPs. The central channel of the NPC functions as a permeability barrier between cyto- and nucleoplasm. The FG-repeat-containing NUPs within the central channel constitute a permeability barrier that allows the passive diffusion of small molecules, while limiting the passage of macromolecules larger than ～40 kDa and enabling nucleocytoplasmic exchange. It thus plays the role of a regulator of intracellular molecule trafficking, constituting an important gatekeeper for macromolecular transports between the nucleus and cytoplasm (Li et al., 2016).

In addition to their main function in nucleocytoplasmic transport, NPCs and their components have been shown to play important roles in many biological processes, such as kinetochore and spindle assembly, cell cycle control, regulation of gene expression, chromatin organization, DNA repair, and DNA replication (Capelson and Hetzer 2009; Capelson et al., 2010; Strambio-De-Castillia et al., 2010; Wozniak et al.,

2010; Van de Vosse et al., 2011; Bukata et al., 2013). In Arabidopsis, NUPs are also involved in multiple biological processes, including flowering and immune responses (Gu et al., 2016; Cheng et al., 2020).

Changing environmental conditions necessitate rapid adaptation of cytoplasmic and nuclear protein content, and a number of key transcription factors are regulated by a rapid nuclear accumulation in response to a signal (Cartwright and Helin, 2000). These TFs must be transported from the cytoplasm to the nucleus to reach their targets and induce or repress their transcription, and exported from the nucleus to the cytoplasm.

Nitrogen (N) is a crucial macronutrient, and N availability in the soil can be a limiting factor for plant growth and development (Marschner et al., 1995). Thus, plants evolved mechanisms to sense and promptly adapt to fluctuating nitrate availability. Importantly, nitrate is not only a nutrient, but also a signaling molecule (Crawford, 1995; Scheible et al., 1997). The rapid transcriptional response to nitrate supply triggers expression changes of thousands of genes.

Members of the Nin Like-Protein (NLP) family are top tier TFs of the nitrate signaling pathway through inducing a cascade of transcriptional regulation (reviewed in Mu and Luo, 2019). The Arabidopsis NLP7 TF is regulated by a very rapid nuclear accumulation within seconds after exposure to nitrate. This mechanism involves the phosphorylation of an evolutionarily conserved Serine by three CALCIUM-DEPENDENT PROTEIN KINASEs (CPK10, CPK30, CPK32, Liu et al., 2017). In addition, NLP7 activity is directly regulated by nitrate binding to its N-terminal region (Liu et al., 2022). The Arabidopsis genome encodes nine NLPs that bind in yeast the nitrate-responsive cis-element (NRE), a conserved DNA sequence motif found in the proximal regions of promoters of nitrate-responsive genes and shown to be necessary and sufficient for their nitrate-induced gene expression (Konishi and Yanagisawa, 2011, 2013). NLP7 was shown as a major TF governing the early nitrate response (Marchive et al., 2013; Konishi and Yanagisawa, 2019; Alvarez et al., 2020). NLP6, the closest homolog of NLP7, exhibits a partially redundant function to that of NLP7. However, although the loss of NLP7 is sufficient to cause a growth reduction under ample nitrate-supply and impaired induction of nitrate-responsive gene, the additional loss of function of NLP6 leads to a stronger phenotype than that of the single mutant *nlp7*-1 (Guan et al., 2017, Cheng et al., 2023). Recent studies demonstrated that NLP2

orchestrates both N and carbon assimilation in response to external nitrate availability (Konishi et al., 2021; Durand et al., 2023). Other NLPs also contribute to the regulation of nitrate-inducible gene expression and nitrate-dependent promotion of vegetative growth in Arabidopsis (Konishi et al., 2021; Liu et al., 2022). The functionality of NLPs is further enriched by their ability to form homo-, heterodimer, or to interact with other proteins via their PB1 domain (Guan et al., 2017; Konishi et al., 2021).

By exploring NLP7 interacting proteins, we discovered that nucleoporins NUP98A and NUP98B interact directly with NLP7. Here, our goal was to elucidate how NUP98A/B bridges nitrate signaling to the NPC function. We first confirmed the interaction of NUP98A/B with NLP7 *in planta*. Then, applying genetics, we showed that the double mutant *nup98a/b* has a higher sensitivity to nitrate limitation and that the loss of function of NUP98A in the *nlp7* mutant background leads to a strongly impaired early transcriptional nitrate response and impaired growth on nitrate fertilisation. Finally, the significant reduction of GFP-NLP7 nuclear accumulation in response to nitrate in the genetic background of *nup98anup98b* strongly underscores the critical role of NUP98A/B proteins in regulating nitrate-dependent nuclear accumulation of NLP7.

Materials and Methods

Plant materials

All Arabidopsis material is in the Col-0 background. The *Arabidopsis thaliana* mutant *nlp7-1* (SALK_26134) derived from T-DNA–mutagenized populations of the Col-0 accession (Alonso-Blanco et al., 2003, Castaings et al., 2009) and was backcrossed twice to Col-0. All mutant seeds were obtained from the NASC, and homozygous lines were identified by genotyping using the primers listed in Supplemental Table S1. Homozygote lines of *nup98a1* (SALK_103803, Jiang et al., 2019), *nup98a2* (SALK_015016, Jiang et al., 2019, also named *dra2-4*, Gallemi et al., 2016), *nup98b1* (GABI_288A08, Jiang et al, 2019), and *nup98b2* (SALK_132527) have been selected by genotyping. The higher-order mutants with and without the *NLP7pro:GFP-NLP7* construct have been obtained by crosses of line A4.4 (Castaings et al., 2009) followed by selfing of the F1 generation, genotyping the F2 generation and selecting for homozygous transgene by hygromycin selection in F3.

Bimolecular Fluorescence Complementation (BiFC)

Open reading frames (without stop codon) flanked by AttB1 and AttB2 sites were amplified from Arabidopsis cDNA clones (Columbia accession) using the primers as given in Supplemental Table S1, cloned into Gateway vector pDONR207 using BP recombination (Invitrogen), and sequenced, except *NUP98A,* where the cDNA sequence optimized for *Arabidopsis thaliana* was synthetized and cloned into pTwist ENTR Kozak entry vector by Twist Biosciences (Supplemental Data Set 1). An LR reaction between the entry vector and the complete set of four pBiFP vectors (Azimzadeh et al., 2008) produced the final expression vectors, where coding sequences are cloned in fusion with the N- or C-terminal parts of YFP, either as N-terminal or C-terminal fusions, under the control of the cauliflower mosaic virus 35S promoter.

Modified versions of NLP7 were produced by PCR. For NLP7 without PB1 domain, the region corresponding to 1-863 amino acids was amplified by PCR and cloned into the Gateway vector pDONR207 using BP recombination. For NLP7 without the predicted GAF domain (Chardin et al., 2014), regions corresponding to amino acids 1-159 and 301-959 were amplified separately. The two fragments were fused together by a second PCR, and the resulting fragment flanked by AttB1 and AttB2 sites was cloned into pDONR207. The primer sequences are given in Table S1. A description of the pH2B2:H2B2-mTurquoise construct can be found in Bouchez et al., 2024.

For BiFC interaction assays, the vectors were transformed into *Agrobacterium tumefaciens* strain C58C1(pMP90) (Kámán-Tóth et al., 2018) and co-infiltrated into *Nicotiana benthamiana* leaves. Plants were grown either in fertilized soil in an air-conditioned greenhouse or on sand in a growth chamber under long day conditions (day 22 ^{o}C / night 18 °C, 16h photoperiod, 130-160 µmolm^{-2}s^{-1} light intensity (Systion 32-42 VDC 330mA, 11V). Plants grown in sand culture were watered with a 2 mM nitrate-containing nutrient solution for 29 days, followed by watering for 3 days with a nutrient solution without N after washing the sand with the N-depleted solution or by watering with a 10 mM nitrate nutrient solution. *Agrobacterium* carrying clones of interest were grown overnight at 28°C in 5 ml LB medium with appropriate antibiotics. Aliquots from the overnight cultures were resuspended in 10 mM $MgCl_2$ and 10 mM 2-(N-morpholine)-ethanesulphonic acid (MES), pH 5.6, to obtain a final OD_{600nm} of 0.5 for tobacco leaf infiltration. YFP fluorescence was detected 2-3 days after infiltration.

During that time, plants were watered with either 0 mM or 10 mM nitrate-containing nutrient solution. Ion equilibrium of the nutrient solution was ensured by replacing KNO_3 and $Ca(NO_3)_2$ with KCl and $CaSO_4$, respectively.

Yeast Two-Hybrid Assays

Coding sequences of *NLP7* and *NUP98A* cloned in pDONR207 were recombined into the pGBKT7 and pGADT7 vectors (Clontech) via LR Clonase reactions and co-transformed into the *Saccharomyces cerevisiae* strain MaV203 (Invitrogen). Yeast was cultured on YPDA plates (Clontech) at 28 °C. For transformation, an overnight liquid culture at OD_{600nm} =0.6 was harvested, resuspended in 1 mL sterile water, pelleted by centrifugation (maximum speed, 15 s), and resuspended in 1 mL of 0.1 M lithium acetate in 1X TE buffer. Transformation mixes contained 5 µg of each plasmid, 5 µL of carrier DNA (Finnzymes, Fisher Scientific), 0.1 mL of yeast suspension, and 0.6 mL of 40% [v/v] PEG 4000 in 0.1 M lithium acetate/1X TE. After a 30 min incubation at 28 °C, mixtures were heat-shocked at 42 °C for 25 min. Cells were pelleted (15 s, max speed), resuspended in 0.25 mL sterile water, and plated on SD/-Trp-Leu selective medium (Clontech). To assess protein–protein interactions, cotransformed colonies were resuspended in 0.1 mL sterile water, and 10 µL was spotted on SD/-Trp-Leu-His plates supplemented with various concentrations of 3-amino-1,2,4-triazole (3-AT). Growth under these conditions was interpreted as a positive interaction.

Growth conditions of Arabidopsis plants

Seeds were stratified for 5 days at 4°C in the dark and then grown either on non-fertilized soil (Stender) or on sand, both supplemented with nutrient solutions (Loudet et al., 2003) containing either 0.5 mM (growth-limiting nitrate supply) or 5 mM (non-limiting nitrate supply) nitrate, in short-day photoperiod with an 8-h light/16-h dark cycle at 21°C/18°C, respectively, 65% relative humidity, and a constant 150 µmol m^{-2} s^{-1} irradiation with Osram 36w light sources. For N limitation conditions, ion equilibrium of the medium was ensured by partly replacing KNO_3 and $Ca(NO_3)_2$ with KCl and $CaSO_4$, respectively.

For nitrate response assays, both for the determination of steady state mRNA levels and confocal analyses, seeds were stratified for 3 days at 4°C and then grown in liquid medium containing 0.07% (w/v) MES pH 5.8, 1 mM KH_2PO_4, 0.5 mM $MgCl_2$, 0.5 mM

$CaSO_4$, microelements as in (Estelle and Somerville, 1987), 0.25% (w/v) sucrose and 3 mM KNO_3 for 10 days in long-day photoperiod (16-h light/8-h dark) at 25°C with a light intensity of 80 µmol photons·m^{-2}·s^{-1} by Philips F17T8/TL741 light sources. For gene expression analysis after 7 days of growth, the medium was changed to fresh medium every 2 days. Eleven-day-old seedlings were then nitrogen-starved for 3 days using fresh medium containing 3 mM KCl instead of 3 mM KNO_3. After 3 days of N starvation, 3 mM nitrate was added for the indicated time periods, and harvests were performed at several time points. For confocal analysis, seedlings were grown as in Marchive et al. (2013) for five days on a 3 mM KNO_3 liquid medium, then N-starved for two days by exchanging the culture medium with an N-free medium in which KNO_3 was replaced by KCl.

Confocal Imaging

Laser scanning confocal imaging was performed using the SP8 confocal laser microscope (Leica, Germany) equipped with an argon laser (488 nm for GFP excitation, intensity 20%) and an argon laser (514 nm for YFP excitation, intensity 20%). Emission was collected at 505 to 525 nm (GFP, gain= 500) or at 520 to 540 nm (YFP, gain= 500). The images were coded green for both GFP and YFP. Images were processed with ImageJ. Plant samples were mounted in 40 µL of a top agar solution (0.1%, w/v). During confocal imaging, 5 µL of 0.5 M KNO_3 was added by capillarity to the mounting medium (45µl).

Gene expression analysis

Measurements of relative steady-state mRNA levels were performed on seedlings (plants at 1.02 developmental growth stages (Boyes et al., 2001)) that had been cultivated in liquid medium as described above. Each sample was shock frozen after harvest and was composed of 26-34 seedlings. Total RNA was extracted using the RNeasy plant mini kit (QIAGEN), including a DNase treatment according to the manufacturer's instructions, or by Trizol method (Invitrogen). First-strand cDNAs were synthesized according to Daniel-Vedele and Caboche (1993) using Moloney murine leukemia virus reverse transcriptase and oligo(dT)15 primers (Promega) or using the SuperScript III Fast strand synthesis system (Invitrogen).

cDNAs were first checked by PCR for contamination by genomic DNA, then relative expression was determined in 384-well plates with a QuantStudio 5 System device (40 3-step cycles; step 1, 95°C, 5 s; step 2, 58°C, 30 s; step 3, 72°C, 30 s) using Takyon qPCR kit for SYBR assay (Eurogentec) (2.5 µL TAKYON SYBR 2X, 0.015 µL Forward primer 100 µM, 0.015 µL Reverse primer 100 µM, 2.5 µL cDNA 1/20 per well). Relative expression was calculated according to the $2^{-\Delta Ct}$ method. Target gene expression was normalized to the geometric mean of the expression of two plant genes, *ACTIN2* (At3g18780) and *TIP41 (*At4g34270*).* All primer sequences are given in Supplemental Table S1.

Statistical analyses

Data were analyzed using non-parametric tests due to non-normal distributions and/or unequal variances. Comparisons between multiple groups were performed using the Kruskal–Wallis test. When a significant difference was detected ($p < 0.05$), Dunn's post hoc test was used for pairwise comparisons without correction for multiple testing. Statistical analyses were conducted in Python using the scipy and scikit-posthocs libraries.

RESULTS

NLP7 protein interacts with the nucleoporin NUP98A/B

Using a Y2H approach (performed by Hybrigenics), we found an interaction between the full-length NLP7 protein and NUP98A. We then confirmed this interaction by pairwise Y2H assay (Figure 1A) and *in planta* by co-expressing ^{C}YFP-NLP7 and ^{N}YFP-NUP98A in *Nicotiana benthamiana.* The YFP signal indicating an interaction between the co-expressed proteins was present in the nucleus as well as in the cytoplasm (Figure 1B-G).

We then tested whether the closely related nucleoporin NUP98B also interacts with NLP7 after transient expression in *N. benthamiana,* using two other nucleoporins, NUP96 and CPR5, as negative controls (Figure 2). NLP7 showed interaction with NUP98B with a localization of the interaction similar to NUP98A (Figure 2D-F),

whereas NUP96 and CPR5 showed no interaction with NLP7 (Figure 2G-L). Taken together, these results demonstrate that the interaction between NLP7 and NUP98A/B is specific to these two NUPs and is not a general interaction with proteins of the NPCs.

PB1 and GAF domains of NLP7 are not essential for NLP7-NUP98A interaction

NLPs contain 2 protein-protein interaction domains. The C-terminal PB1 domain, which has been shown to be involved in the formation of homo- and heterodimers of NLP proteins (Konishi and Yanagisawa, 2019) and with proteins that do not contain PB1 domains (Guan et al., 2017). The second, the N-terminal GAF-like domain, is reported as a protein-protein interacting domain (Ho et al., 2000; Wu et al., 2022). To identify the NLP7 protein domains involved in the interaction with NUP98A, we produced NLP7 constructs without either the GAF-like domain or the PB1 domain. NLP7 without either GAF or PB1 domain interacted with NUP98A in the BIFC assays, producing positive signal both in the nucleus and in the cytoplasm (Supplemental Figure S1). Thus, the NLP7 PB1 and GAF domains might contribute to the interaction between NLP7 and NUP98A/B but are not essential for it.

The intracellular localization of the NUP98A-NLP7 interaction is modified by the N status of the plants

NLP7 accumulates in the nucleus in the presence of nitrate and is localized in the cytosol in N-starved seedlings (Marchive et al., 2013). Because NUP98A/B are key components of the NPC, we then ask whether their association with NLP7 might depend on the N status. We studied the interaction between NLP7 and NUP98A in *N. benthamiana* plants that have been grown under ample nitrate supply (10 mM) and in plants that were treated with a 5-day N depletion. In addition, leaf discs from N-depleted plants were resupplied with nitrate 10 min before observation (Figure 3). The fluorescent signal indicating the interaction between NLP7 and NUP98A was present both in the cytoplasm and in the nucleus in all three conditions, however, in the case of the starved leaves, the nuclear signal was less defined (Figure 3 D-F). Quantification of the fluorescence ratio between nucleus and cytoplasm confirmed these observations (Figure 3 J). Our results suggest that NUP98A/B interact with NLP7s when both proteins are localized in the same cellular compartment.

Limiting nitrate supply amplifies the early senescence of nup98anup98b double mutants

The protein interaction of NLP7 with NUP98A/B led us to assess the physiological role of the NUP98A/B-dependent response to nitrate availability. We analyzed the growth of NUP98A/B loss-of-function mutants (*nup98a-1, nup98a-2, nup98b-1, nup98b-2* and *nup98a-1nup98b-1*) under contrasting nitrate supply that had revealed nitrate-dependent growth phenotypes of *nlp7* and *nlp2* mutants (Durand et al., 2023). We grew the mutants in sand culture under short-day conditions (8 h light/16 h dark) with either 0.5 mM nitrate or 5 mM nitrate supply for 39 days and determined rosette and root biomass (Figure 4A - D). Under both N supply conditions, the rosette and root biomass of *nup98a* and *nup98b* single mutants was similar to that of the wild type (WT) Col-0. Under non-limiting N supply, WT plants displayed the expected (2.5-fold) increase in rosette fresh weight compared to WT plants grown under 0.5 mM N supply (Figure 4A and B). Rosette biomass of the double mutant *nup98a-1nup98b-1* was strongly decreased in both N regimes (by 72 and 84 % under 0.5 and 5mM nitrate supply, respectively) with an early senescence phenotype that was described before for this double mutant (Xiao et al., 2020). Root fresh weight of *nup98a* and *nup98b* mutants was also similar to WT, with a trend towards slightly lower root biomass compared to WT under limiting N supply (Figure 4 C and D). Root biomass was also decreased in the case of the double mutant, and the rosette/root ratio was modified for the double mutant compared to WT. Interestingly, it decreased slightly by 30% under non-limiting N supply, but increased 2-fold under limiting N supply. The shoot/root ratio is an indicator of N limitation, suggesting that the double mutant experienced less N limitation than the WT and the single mutants under limiting N supply. Remarkably, the senescence phenotype of *nup98a-1nup98b-1* double mutant that was visible by the loss of chlorophyll, particularly in older leaves, had appeared much earlier in plants grown under nitrate-limiting conditions than under ample nitrate supply (at 28, 35 and 38 days, respectively, Figure 4, G and H). Taken together, these observations suggest that NUP98A/B are necessary to prevent early N limitation-induced senescence.

Double and triple mutant phenotypes support an interplay between NLP7 and NUP98A/B

To study the genetic interaction of NUP98A/B and NLP7 and to further unravel the roles played by NUP98A/B in the NLP7-dependent nitrate responses, we generated the *nup98a-1nlp7-1 and nup98b-1nlp7-1* double mutants and the triple mutant *nup98a-1nup98b-1nlp7-1.*

We first studied the growth of single and higher order mutants in comparison to the WT in sand culture under low and ample nitrate supply in short day conditions (Figure 5 A-C). Under limiting N supply, the single mutants *nup98a*, *nup98b* and *nlp7-1* attained a rosette biomass comparable to that of the WT, as expected. The rosette FW of the double mutants *nlp7-1nup98a* and *nlp7-1nup98b* decreased by 40% and 30% respectively, compared to *nlp7-1.* The double mutant *nup98anup98b* had a rosette biomass of 37 mg, corresponding to 22% of WT and the triple mutant *nup98a-1nup98b-1nlp7-1* barely attained an FW of 1 mg (Figure 5A). Under non-limiting nitrate supply, whereas the *nup98a* and *nup98b* showed no difference to WT, the biomass of the *nlp7-1* mutant was decreased 2-fold compared to WT, as reported previously *and* explained by a constitutive N-limitation phenotype under ample nitrate supply (Castaings et al., 2009). In these conditions, rosette biomass of the double mutants *nlp7-1nup98a* and *nlp7-1nup98b* was decreased by 50% and 35%, respectively, compared to *nlp7-1*, thus slightly stronger than under limiting nitrate supply. The triple mutant reached a biomass of 5.5 mg compared to 75 mg of the double mutant *nup98anup98b.* Together, our data suggest that both NLP7 and NUP98A/B determine plant growth in response to N supply. This can be due either to their participation in a shared regulatory pathway or to two different pathways affecting growth in response to the N status of the plant.

Loss of function of both NLP7 and NUP98 amplified the impaired PNR of *nlp7-1* mutants

Given the conserved role of nucleoporine and transcription factor in many eukaryotes, the interaction between NLP7 and NUP98A/B may reflect a broader principle whereby nuclear transport components cooperate with transcriptional regulators to fine-tune N responses. We compared steady state levels of mRNA in seedlings either grown for

11 days on 3 mM nitrate medium, or submitted to 3 days of N starvation after 11 days on 3 mM nitrate, or resupplied for 30 min by 3 mM nitrate after the 3-day starvation period. We measured by RT-qPCR the relative transcript levels of 18 NLP7-dependent nitrate-regulated genes in *nlp7-1nup98a* double mutants compared to the single mutants and the WT (Figure 5 D-G). The main difference between *nlp7-1* and the double mutant *nlp7-1nup98a* has been observed after nitrate resupply. For all of the studied genes, the nitrate-triggered increase in steady-state transcript level was diminished for *nlp7-1* as expected. For the double mutant *nlp7-1nup98a*, this reduced increase was further diminished in the case of *NITRATE TRANSPORTER 2.1* (*NRT2.1)*, *NRT2.2*, *NLP1*, *NITRITE REDUCTASE* (NII), *NITRATE REDUCTASE1* (*NIA1*), *NAR2*, and *HRS1 HOMOLOGOUS 1* (*HHO1)*. A similar tendency was observed for *LOB BINDING DOMAIN 38* (*LBD38*), *NLP2* and *BTB/POZ AND TAZ DOMAIN-CONTAINING PROTEIN 5* (*BT5*), whereas no difference in the expression level after 30 min of nitrate resupply for the double mutant compared to *nlp7-1* was found for *MAP KINASE KINASE KINASE* 14 (*MAP3K14)*, *MAP3K13*, *NLP3*, *BT2*, *HYPERSENSITIVITY TO LOW PI-ELICITED PRIMARY ROOT SHORTENING 1* (*HRS1)*, *LBD39*, *NIA2* and *NRT1.1*. Taken together, for several nitrate-regulated genes, combining *nlp7* and *nup98* mutations resulted in an additive abolishment of nitrate induction, probably due to the consequences of impaired nuclear accumulation of other NLPs or other TFs required for a complete PNR.

NUP98A and NUP98B are required for the nitrate-triggered nuclear accumulation of NLPs

To decipher the mechanism underlying the various morphological and molecular phenotypes of the higher-order mutants, we studied the nuclear accumulation of GFP-NLP7 in response to nitrate resupply to N-depleted seedlings in different mutant backgrounds. We hypothesized that the interaction of NUP98A and NUP98B with NLP7 is required for the nitrate-triggered nuclear accumulation and NLP7-dependent nitrate-regulated gene expression and growth.

We introduced the GFP-NLP7 translation fusion driven by the NLP7 promoter into these NUP98 loss of function mutants by crossing an *NLP7pro:GFP-NLP7* (*nlp7-1*) transgenic line (Castaings et al., 2009) with the single mutant *nup98a-1* and the double mutant *nup98a-1nup98b-1*. In N-depleted 10-day-old seedlings, GFP-NLP7 was

localized in the cytosol of all genotypes (Figure 6 A, C, E). At 10 minutes after nitrate resupply, in the presence of NUP98A and NUP98B GFP-NLP7 accumulated rapidly in the nucleus (Figure 6 B). The loss of function of NUP98A was accompanied by a decrease in the accumulation in the nucleus after nitrate resupply (Figure 6 D). In the absence of both NUP98A and NUP98B, the accumulation of GFP-NLP7 in the nucleus in response to nitrate resupply was almost abolished (Figure 6 F). Quantification of the fluorescence ratio between nucleus and cytoplasm confirmed these observations (Figure 6 G). Thus, our results indicate a specific role of NUP98A/B for the nitrate-triggered nuclear accumulation of NLP7.

Discussion

Nucleoporins are increasingly recognized not only as structural components of the nuclear pore complex (NPC) but also as active regulators of gene expression and signaling pathways across eukaryotes. In this study, we uncover a novel role for the plant nucleoporins NUP98A and NUP98B in controlling the nuclear accumulation of the transcription factor NLP7, a central regulator of nitrogen signaling. While NUP98 proteins are generally thought to maintain NPC integrity and mediate nucleo-cytosolic trafficking (Tamura et al., 2010; Raveh et al., 2016), studies in yeast, animals, and plants have highlighted their mobility and functional versatility beyond nuclear transport (Capitanio et al., 2017; Gallemí et al., 2016). Our work now extends this paradigm to nitrogen signaling in plants.

Here, we report a novel role for the nucleoporins NUP98A and NUP98B in regulating the nuclear accumulation of the TF NLP7. Based on their sequence homology with other species, plant NUP98A/B are considered to be required for maintaining the NPC structure and facilitating macromolecule nucleo-cytosolic trafficking (Tamura et al., 2010; Raveh et al., 2016). Although they have an important structural role in the NPC, NUP98s in yeast, animals and plants are mobile proteins that can be localized in different cellular compartments (Capitanio et al., 2017; Gallemí et al., 2016). This has various implications for their role in other biological processes. We validated the interaction between NUP98A and NLP7 using *in planta* BiFC assays, confirming the results obtained through yeast two-hybrid screening. Interaction was detected both in

the cytosol and the nucleus. We cannot exclude that the strong transient expression of the splitYFP proteins driven by the CaMV 35S promoter leads to a protein localization different from the native conditions. However, the localization of the interacting complex corresponded to the localization of NLP7 tagged with GFP under the particular condition, as in N-depletion condition, the interaction in the nucleus was less pronounced, as expected from the NLP7 localisation change under this condition (Marchive et al., 2013).

Here, we showed that neither the NLP7 GAF domain nor its PB1 domain is essential for the interaction with NUP98A/B, however, it is possible that both domains act redundantly to ensure this interaction. Found in a variety of proteins, including TFs, the GAF domain is important for protein-protein interactions and can bind a variety of ligands, including cGMP, cAMP, and small molecules such as oxygen and nitrate (Ho et al., 2000; Moglich et al., 2009; Niemann et al., 2014; Su and Lagarias, 2007; Grefen et al., 2008). It has been shown that the NLP7 PB1 domain is important for its interaction with other NLPs, but also with the transcription factor teosinte branched1/cycloidea/proliferating cell factor20 (TCP20), and SUCROSE NON-FERMENTING 1-RELATED KINASE 1 (SnRK1) (Konishi and Yanagisawa, 2019; Guan et al., 2017; Wang et al., 2022). The NLP7 protein possesses short intrinsic disordered regions (IDRs), which leads to the hypothesis that these IDRs interact with the FG motifs of NUP98. However, the nature of the underlying molecular interactions between FG repeats that might lead to protein condensates (Ahn et al., 2025)is largely unknown. Interestingly, it has been shown recently that protein condensation is involved in the specificity of transport through the NPC (Wang et al., 2023).

Despite the high probability that the positive BiFC between NLP7 and NUP98A/B is due to a direct interaction between these proteins, we cannot exclude that a third partner is necessary for the interaction. For example, NirA, the specific transcription factor of the nitrate assimilation pathway of *Aspergillus nidulans*, interacts with the nuclear export factor KapK, which bridges an interaction with a nucleoporin-like protein. Interestingly, NirA, which has no structural homology with NLP7, also accumulates in the nucleus upon induction by nitrate via a nuclear retention mechanism (Bernreiter et al., 2007).

Several other *nup* mutants are, like *nup98anup98b*, also modified for the intracellular partitioning of regulatory proteins, including TFs. For example, the mutation of the HIGH EXPRESSION OF OSMOTICALLY RESPONSIVE GENES 1 (HOS1) reduces the nuclear accumulation of SnRK1a1 (Margalha et al., 2023) and of PHYTOCHROME-INTERACTING FACTOR 4 (PIF4) (Zhang et al., 2020). The NUP62-subcomplex modulates Flowering locus C (FLC) nuclear import, and NUP85 is a player in the nuclear-cytosolic trafficking of A*CQOS*, encoding a nucleotide-binding leucine-rich repeat (NLR) protein (Mori et al., 2024). The nuclear-cytosolic partitioning of these proteins is regulated by abiotic stresses or the transition to flowering. Here, we show that the response to nutrient availability is also governed by the function of a NUP, NUP98A/B.

nup98anup98b double mutants display early flowering (Jiang et al., 2019) with early senescence during flowering. NUP98A/B are also involved in the control of starch degradation (Xiao et al., 2020) and in the circadian control (Jiang et al. 2019, 2020). Here, we found that single *nup98a* mutants had only minor phenotypes, whereas the *nup98anup98b* double mutants showed a severe growth phenotype associated with early senescence as reported before (Xiao et al., 2020). Interestingly, the early senescence is exacerbated by N limitation. *nlp7* mutants display several traits of N limitation, despite growing under non-limiting nitrate supply (Castaings et al., 2009). Whereas this does not lead to early senescence of the *nlp7* mutants, impaired nuclear accumulation of other NLPs in the *nup98anup98b* mutant might lead to its early senescent phenotype under N limitation. Indeed, our study shows that in *nup98a-1nlp7-1* double mutants, a subset of nitrate-regulated genes displayed reduced transcript abundance in response to nitrate resupply compared to the *nlp7* mutant. This might be due to the impact of the loss of function of NUP98A on the activities of other TFs involved in nitrate signalling, including NLP1/2/6/7 (Konishi et al., 2021, Cheng et al., 2023).

Besides the pivotal role in gating nuclear and cytoplasmic functions, the nuclear pore proteins function in key biological processes, including chromatin tethering to the nuclear periphery, a mechanism contributing to the regulation of gene expression (Ungricht and Kutay, 2017; Smith et al., 2015). Thus, it will require further

investigations to determine whether NUP98A/B act with NLP to orchestrate the nitrate-triggered transcriptional regulation of nitrate-regulated genes by facilitating their transcriptional activation by NLPs in addition to regulating nuclear accumulation of NLPs in response to nitrate.

Interestingly, in humans, NUP98 has oncogenic roles as a genetic fusion partner (Gough et al., 2011). Indeed, in malignant cells, NUP98 occurs as part of fusion proteins with TFs, pointing to the involvement of NUP98 in transcriptomic dysregulation during oncogenesis. In plants, such NUP98 fusion proteins have not been reported, and it can be speculated that instead, protein-protein interactions evolved. Further studies are required to reveal further regulatory mechanisms governed by the NUP98-NLP7 protein complex.

In conclusion, this study demonstrates that in Arabidopsis, NUP98A/B promotes NLP7 activity through the control of its nucleocytoplasmic trafficking and thereby impacts the rapid transcriptional response to nitrate availability and the acclimation of plant growth to nitrate supply.

Acknowledgments

We thank Hervé Ferry, Jean-Christophe Guedet and Philippe Maréchal for plant care, Gladys Cloarec for support for confocal analyses, and Alizée Teinturier for technical assistance. We also thank the NASC and ABRC for supplying Arabidopsis T-DNA insertion lines. This work has benefited from the support of IJPB's Plant Observatory technological platforms PO-Plants and PO-Cyto and was supported by ANR NITRASENSE (ANR-16-CE20-022, ZK, AK). The IJPB benefits from the support of the Saclay Plant Sciences (SPS) Network (ANR-17-EUR-0007). We thank Sylvie Ferrario-Méry, Thomas Girin, Anne-Sophie Leprince and Christian Meyer for fruitful discussions.

References

Ahn, J.H., Guo, Y., Lyons, H., Mackintosh, S.G., Lau, B.K., Edmondson, R.D., Byrum, S.D., Storey, A.J., Tackett, A.J., Cai, L., Sabari, B.R., Wang, G.G., 2025. The phenylalanine-and-glycine repeats of NUP98 oncofusions form

condensates that selectively partition transcriptional coactivators. Mol Cell 85, 708-725.e9. https://doi.org/10.1016/j.molcel.2024.12.026

Alonso-Blanco, C., Bentsink, L., Hanhart, C.J., Blankestijn-de Vries, H., Koornneef, M., 2003. Analysis of natural allelic variation at seed dormancy loci of Arabidopsis thaliana. Genetics 164, 711–729. https://doi.org/10.1093/genetics/164.2.711

Alvarez, J.M., Schinke, A.-L., Brooks, M.D., Pasquino, A., Leonelli, L., Varala, K., Safi, A., Krouk, G., Krapp, A., Coruzzi, G.M., 2020. Transient genome-wide interactions of the master transcription factor NLP7 initiate a rapid nitrogen-response cascade. Nature Communications 11, 1157. https://doi.org/10.1038/s41467-020-14979-6

Azimzadeh, J., Nacry, P., Christodoulidou, A., Drevensek, S., Camilleri, C., Amiour, N., Parcy, F., Pastuglia, M., Bouchez, D., 2008. Arabidopsis TONNEAU1 proteins are essential for preprophase band formation and interact with centrin. The Plant Cell 20, 2146–2159. https://doi.org/10.1105/tpc.107.056812

Bernreiter, A., Ramon, A., Fernández-Martínez, J., Berger, H., Araújo-Bazan, L., Espeso, E.A., Pachlinger, R., Gallmetzer, A., Anderl, I., Scazzocchio, C., Strauss, J., 2007. Nuclear export of the transcription factor NirA is a regulatory checkpoint for nitrate induction in Aspergillus nidulans. Molecular and Cellular Biology 27, 791–802. https://doi.org/10.1128/MCB.00761-06

Bouchez, D., Uyttewaal, M., Pastuglia, M., 2024. Spatiotemporal regulation of plant cell division. Curr Opin Plant Biol 79, 102530. https://doi.org/10.1016/j.pbi.2024.102530

Boyes, D.C., Zayed, A.M., Ascenzi, R., McCaskill, A.J., Hoffman, N.E., Davis, K.R., Görlach, J., 2001. Growth stage-based phenotypic analysis of Arabidopsis: a model for high throughput functional genomics in plants. The Plant Cell 13, 1499–1510. https://doi.org/10.1105/tpc.010011

Bukata, L., Parker, S.L., D'Angelo, M.A., 2013. Nuclear pore complexes in the maintenance of genome integrity. Current Opinion in Cell Biology 25, 378–386. https://doi.org/10.1016/j.ceb.2013.03.002

Capelson, M., Hetzer, M.W., 2009. The role of nuclear pores in gene regulation, development and disease. EMBO reports 10, 697–705. https://doi.org/10.1038/embor.2009.147

Capelson, M., Liang, Y., Schulte, R., Mair, W., Wagner, U., Hetzer, M.W., 2010. Chromatin-bound nuclear pore components regulate gene expression in

higher eukaryotes. Cell 140, 372–383. https://doi.org/10.1016/j.cell.2009.12.054

Capitanio, J.S., Montpetit, B., Wozniak, R.W., 2017. Human Nup98 regulates the localization and activity of DExH/D-box helicase DHX9. Elife 6, e18825. https://doi.org/10.7554/eLife.18825

Cartwright, P., Helin, K., 2000. Nucleocytoplasmic shuttling of transcription factors. Cellular and molecular life sciences: CMLS 57, 1193–1206. https://doi.org/10.1007/pl00000759

Castaings, L., Camargo, A., Pocholle, D., Gaudon, V., Texier, Y., Boutet-Mercey, S., Taconnat, L., Renou, J.-P., Daniel-Vedele, F., Fernandez, E., Meyer, C., Krapp, A., 2009. The nodule inception-like protein 7 modulates nitrate sensing and metabolism in Arabidopsis. The Plant Journal: For Cell and Molecular Biology 57, 426–435. https://doi.org/10.1111/j.1365-313X.2008.03695.x

Chardin, C., Girin, T., Roudier, F., Meyer, C., Krapp, A., 2014. The plant RWP-RK transcription factors: key regulators of nitrogen responses and of gametophyte development. Journal of Experimental Botany 65, 5577–5587. https://doi.org/10.1093/jxb/eru261

Cheng, Y.-H., Durand, M., Brehaut, V., Hsu, F.-C., Kelemen, Z., Texier, Y., Krapp, A., Tsay, Y.-F., 2023. Interplay between NIN-LIKE PROTEINs 6 and 7 in nitrate signaling. Plant Physiology 192, 3049–3068. https://doi.org/10.1093/plphys/kiad242

Cheng, Z., Zhang, X., Huang, P., Huang, G., Zhu, J., Chen, F., Miao, Y., Liu, L., Fu, Y.-F., Wang, X., 2020. Nup96 and HOS1 Are Mutually Stabilized and Gate CONSTANS Protein Level, Conferring Long-Day Photoperiodic Flowering Regulation in Arabidopsis. The Plant Cell 32, 374–391. https://doi.org/10.1105/tpc.19.00661

Crawford, N.M., 1995. Nitrate: nutrient and signal for plant growth. The Plant Cell 7, 859–868. https://doi.org/10.1105/tpc.7.7.859

Daniel-Vedele, F., Caboche, M., 1993. A tobacco cDNA clone encoding a GATA-1 zinc finger protein homologous to regulators of nitrogen metabolism in fungi. Mol Gen Genet 240, 365–373. https://doi.org/10.1007/BF00280388

Durand, M., Brehaut, V., Clement, G., Kelemen, Z., Macé, J., Feil, R., Duville, G., Launay-Avon, A., Roux, C.P.-L., Lunn, J.E., Roudier, F., Krapp, A., 2023. The Arabidopsis transcription factor NLP2 regulates early nitrate responses and integrates nitrate assimilation with energy and carbon skeleton supply. The Plant Cell 35, 1429–1454. https://doi.org/10.1093/plcell/koad025

Estelle, M.A., Somerville, C., 1987. Auxin-resistant mutants of Arabidopsis thaliana with an altered morphology. Mol Gen Genet 206, 200–206. https://doi.org/10.1007/BF00333575

Gallemí, M., Galstyan, A., Paulišić, S., Then, C., Ferrández-Ayela, A., Lorenzo-Orts, L., Roig-Villanova, I., Wang, X., Micol, J.L., Ponce, M.R., Devlin, P.F., Martínez-García, J.F., 2016. DRACULA2 is a dynamic nucleoporin with a role in regulating the shade avoidance syndrome in Arabidopsis. Development (Cambridge, England) 143, 1623–1631. https://doi.org/10.1242/dev.130211

Gough, S.M., Slape, C.I., Aplan, P.D., 2011. NUP98 gene fusions and hematopoietic malignancies: common themes and new biologic insights. Blood 118, 6247–6257. https://doi.org/10.1182/blood-2011-07-328880

Grefen, C., Städele, K., Růzicka, K., Obrdlik, P., Harter, K., Horák, J., 2008. Subcellular localization and in vivo interactions of the Arabidopsis thaliana ethylene receptor family members. Molecular Plant 1, 308–320. https://doi.org/10.1093/mp/ssm015

Gu, Y., Zebell, S.G., Liang, Z., Wang, S., Kang, B.-H., Dong, X., 2016. Nuclear Pore Permeabilization Is a Convergent Signaling Event in Effector-Triggered Immunity. Cell 166, 1526-1538.e11. https://doi.org/10.1016/j.cell.2016.07.042

Guan, P., Ripoll, J.-J., Wang, R., Vuong, L., Bailey-Steinitz, L.J., Ye, D., Crawford, N.M., 2017. Interacting TCP and NLP transcription factors control plant responses to nitrate availability. Proceedings of the National Academy of Sciences of the United States of America 114, 2419–2424. https://doi.org/10.1073/pnas.1615676114

Ho, Y.S., Burden, L.M., Hurley, J.H., 2000. Structure of the GAF domain, a ubiquitous signaling motif and a new class of cyclic GMP receptor. The EMBO journal 19, 5288–5299. https://doi.org/10.1093/emboj/19.20.5288

Jiang, S., Xiao, L., Huang, P., Cheng, Z., Chen, F., Miao, Y., Fu, Y.-F., Chen, Q., Zhang, X.-M., 2019. Nucleoporin Nup98 participates in flowering regulation in a CONSTANS-independent mode. Plant Cell Reports 38, 1263–1271. https://doi.org/10.1007/s00299-019-02442-w

Kámán-Tóth, E., Pogány, M., Dankó, T., Szatmári, Á., Bozsó, Z., 2018. A simplified and efficient Agrobacterium tumefaciens electroporation method. 3 Biotech 8, 148. https://doi.org/10.1007/s13205-018-1171-9

Konishi, M., Okitsu, T., Yanagisawa, S., 2021. Nitrate-responsive NIN-like protein transcription factors perform unique and redundant roles in Arabidopsis.

Journal of Experimental Botany 72, 5735–5750. https://doi.org/10.1093/jxb/erab246

Konishi, M., Yanagisawa, S., 2019. The role of protein-protein interactions mediated by the PB1 domain of NLP transcription factors in nitrate-inducible gene expression. BMC plant biology 19, 90. https://doi.org/10.1186/s12870-019-1692-3

Konishi, M., Yanagisawa, S., 2013. Arabidopsis NIN-like transcription factors have a central role in nitrate signalling. Nature Communications 4, 1617. https://doi.org/10.1038/ncomms2621

Konishi, M., Yanagisawa, S., 2011. Roles of the transcriptional regulation mediated by the nitrate-responsive cis-element in higher plants. Biochemical and Biophysical Research Communications 411, 708–713. https://doi.org/10.1016/j.bbrc.2011.07.008

Li, C., Goryaynov, A., Yang, W., 2016. The selective permeability barrier in the nuclear pore complex. Nucleus 7, 430–446. https://doi.org/10.1080/19491034.2016.1238997

Liu, K.-H., Liu, M., Lin, Z., Wang, Z.-F., Chen, B., Liu, C., Guo, A., Konishi, M., Yanagisawa, S., Wagner, G., Sheen, J., 2022. NIN-like protein 7 transcription factor is a plant nitrate sensor. Science (New York, N.Y.) 377, 1419–1425. https://doi.org/10.1126/science.add1104

Liu, K.-H., Niu, Y., Konishi, M., Wu, Y., Du, H., Sun Chung, H., Li, L., Boudsocq, M., McCormack, M., Maekawa, S., Ishida, T., Zhang, C., Shokat, K., Yanagisawa, S., Sheen, J., 2017. Discovery of nitrate-CPK-NLP signalling in central nutrient-growth networks. Nature 545, 311–316. https://doi.org/10.1038/nature22077

Loudet, O., Chaillou, S., Merigout, P., Talbotec, J., Daniel-Vedele, F., 2003. Quantitative Trait Loci Analysis of Nitrogen Use Efficiency in Arabidopsis. Plant Physiol 131, 345–358. https://doi.org/10.1104/pp.102.010785

Marchive, C., Roudier, F., Castaings, L., Bréhaut, V., Blondet, E., Colot, V., Meyer, C., Krapp, A., 2013. Nuclear retention of the transcription factor NLP7 orchestrates the early response to nitrate in plants. Nature Communications 4, 1713. https://doi.org/10.1038/ncomms2650

Margalha, L., Elias, A., Belda-Palazón, B., Peixoto, B., Confraria, A., Baena-González, E., 2023. HOS1 promotes plant tolerance to low-energy stress via the SnRK1 protein kinase. Plant J 115, 627–641. https://doi.org/10.1111/tpj.16250

Marschner, H., 1995. Mineral Nutrition of Higher Plants, 2nd ed. Academic Press, London, England.

Möglich, A., Ayers, R.A., Moffat, K., 2009. Structure and signaling mechanism of Per-ARNT-Sim domains. Structure (London, England: 1993) 17, 1282–1294. https://doi.org/10.1016/j.str.2009.08.011

Mori, K., Murakoshi, Y., Tamura, M., Kunitake, S., Nishimura, K., Ariga, H., Tanaka, K., Iuchi, S., Yotsui, I., Sakata, Y., Taji, T., 2024. Mutations in nuclear pore complex promote osmotolerance in Arabidopsis by suppressing the nuclear translocation of ACQOS and its osmotically induced immunity. Front Plant Sci 15, 1304366. https://doi.org/10.3389/fpls.2024.1304366

Mu, X., Luo, J., 2019. Evolutionary analyses of NIN-like proteins in plants and their roles in nitrate signaling. Cellular and molecular life sciences: CMLS 76, 3753–3764. https://doi.org/10.1007/s00018-019-03164-8

Niemann, V., Koch-Singenstreu, M., Neu, A., Nilkens, S., Götz, F., Unden, G., Stehle, T., 2014. The NreA protein functions as a nitrate receptor in the staphylococcal nitrate regulation system. Journal of Molecular Biology 426, 1539–1553. https://doi.org/10.1016/j.jmb.2013.12.026

Raveh, B., Karp, J.M., Sparks, S., Dutta, K., Rout, M.P., Sali, A., Cowburn, D., 2016. Slide-and-exchange mechanism for rapid and selective transport through the nuclear pore complex. Proceedings of the National Academy of Sciences of the United States of America 113, E2489-2497. https://doi.org/10.1073/pnas.1522663113

Scheible, W.-R., Lauerer, M., Schulze, E.-D., Caboche, M., Stitt, M., 1997. Accumulation of nitrate in the shoot acts as a signal to regulate shoot-root allocation in tobacco. The Plant Journal 11, 671–691. https://doi.org/10.1046/j.1365-313X.1997.11040671.x

Smith, C., Lari, A., Derrer, C.P., Ouwehand, A., Rossouw, A., Huisman, M., Dange, T., Hopman, M., Joseph, A., Zenklusen, D., Weis, K., Grunwald, D., Montpetit, B., 2015. In vivo single-particle imaging of nuclear mRNA export in budding yeast demonstrates an essential role for Mex67p. The Journal of Cell Biology 211, 1121–1130. https://doi.org/10.1083/jcb.201503135

Strambio-De-Castillia, C., Niepel, M., Rout, M.P., 2010. The nuclear pore complex: bridging nuclear transport and gene regulation. Nature Reviews. Molecular Cell Biology 11, 490–501. https://doi.org/10.1038/nrm2928

Su, Y., Lagarias, J.C., 2007. Light-independent phytochrome signaling mediated by dominant GAF domain tyrosine mutants of Arabidopsis phytochromes in

transgenic plants. The Plant Cell 19, 2124–2139. https://doi.org/10.1105/tpc.107.051516

Tamura, K., Fukao, Y., Iwamoto, M., Haraguchi, T., Hara-Nishimura, I., 2010. Identification and characterization of nuclear pore complex components in Arabidopsis thaliana. The Plant Cell 22, 4084–4097. https://doi.org/10.1105/tpc.110.079947

Ungricht, R., Kutay, U., 2017. Mechanisms and functions of nuclear envelope remodelling. Nature Reviews. Molecular Cell Biology 18, 229–245. https://doi.org/10.1038/nrm.2016.153

Van de Vosse, D.W., Wan, Y., Wozniak, R.W., Aitchison, J.D., 2011. Role of the nuclear envelope in genome organization and gene expression. Wiley Interdisciplinary Reviews. Systems Biology and Medicine 3, 147–166. https://doi.org/10.1002/wsbm.101

Wang, H., Han, C., Wang, J.-G., Chu, X., Shi, W., Yao, L., Chen, J., Hao, W., Deng, Z., Fan, M., Bai, M.-Y., 2022. Regulatory functions of cellular energy sensor SnRK1 for nitrate signalling through NLP7 repression. Nature Plants 8, 1094–1107. https://doi.org/10.1038/s41477-022-01236-5

Wang, J., Pei, G., Wang, Y., Wu, D., Liu, X., Li, G., He, J., Zhang, X., Shan, X., Li, P., Xie, D., 2023. Phase separation of the nuclear pore complex facilitates selective nuclear transport to regulate plant defense against pathogen and pest invasion. Molecular Plant 16, 1016–1030. https://doi.org/10.1016/j.molp.2023.04.008

Wozniak, R., Burke, B., Doye, V., 2010. Nuclear transport and the mitotic apparatus: an evolving relationship. Cellular and molecular life sciences: CMLS 67, 2215–2230. https://doi.org/10.1007/s00018-010-0325-7

Wu, X., Han, J., Guo, C., 2022. Function of Nuclear Pore Complexes in Regulation of Plant Defense Signaling. International Journal of Molecular Sciences 23, 3031. https://doi.org/10.3390/ijms23063031

Xiao, L., Jiang, S., Huang, P., Chen, F., Wang, X., Cheng, Z., Miao, Y., Liu, L., Searle, I., Liu, C., Wu, X.-X., Fu, Y.-F., Chen, Q., Zhang, X.-M., 2020. Two Nucleoporin98 homologous genes jointly participate in the regulation of starch degradation to repress senescence in Arabidopsis. BMC plant biology 20, 292. https://doi.org/10.1186/s12870-020-02494-1

Zhang, A., Wang, S., Kim, J., Yan, J., Yan, X., Pang, Q., Hua, J., 2020. Nuclear pore complex components have temperature-influenced roles in plant growth and immunity. Plant Cell Environ 43, 1452–1466. https://doi.org/10.1111/pce.13741

Figures

Figure 1. **NLP7 interacts with NUP98A.**

(A) Yeast two-hybrid assay using NLP7 fused with the binding domain (BD) and NUP98A fused with the DNA activation domain (AD). Cells were grown on selective and non-selective plates.

(B-G) NLP7 interacts with NUP98A in BiFC assays in *N. benthamiana.*

(B, E) YFP fluorescence (green), (C, F) chlorophyll autofluorescence (magenta), (D, G) H2B nuclear marker - mTurcoise fluorescence (blue)

Scale bar = (B-D) 50 µm, (E-F) 5 µm

Figure 2. **NLP7 interacts with NUP98A and NUP98B.**

(A-L) NLP7 interacts with NUP98A and NUP98B in BiFC assays in *N. benthamiana.* (**A-C**) NLP7-NUP98A interaction, (**D-F**) NLP7-NUP98B interaction, **(G-I)** NLP7-CPR5 interaction (negative control), **(J-L)** NLP7-NUP96 interaction (negative control). (**A, D, G, J**) YFP fluorescence (green), (**B, E, H, K**) chlorophyll autofluorescence (magenta) (**C, F, I, L**) YFP fluorescence (green) was merged with chlorophyll autofluorescence (magenta)

Scale bar = 25 µm.

Figure 3. **NLP7 interacts with NUP98A in the nucleus in the presence of nitrate**

(A-I) BiFC assays between NLP7 and NUP98A in *N. benthamiana.* (**A-C**) Plants were supplied with 10 mM nitrate nutrition solution. (**D-F**) Plants have been N-depleted for 5-days. **(G-I)** leaf disc from transiently transformed N-depleted plants were treated for 10 min with nitrate. (A, D, G) YFP fluorescence (green), (B, E, H) chlorophyll autofluorescence (magenta), (C, F, I) YFP fluorescence (green) was merged with chlorophyll autofluorescence (magenta). Scale bar = 50 µm. **(J)** Nuclear-to-cytoplasmic fluorescence intensity ratios in plant cells across different samples. Ratios were calculated from measurements in 13-15 images per sample. Data are presented as boxplots. Statistical significance was assessed using the Kruskal–Wallis test

followed by Dunn's post hoc test for pairwise comparisons. *P*-values: 4.47e-02 (**), 2.7e-07 (***), 1.08e-03 (###).

Figure 4. **Biomass and Shoot/Root ratio of *nup98a/b single and double* mutants grown under limiting and non-limiting nitrate supply.**

Plants were grown on sand under short days with a light intensity of 150 µE for 39 d (**A, B**) Rosette fresh weight of plants grown under limiting (0.5 mM, **A**) and non-limiting (5 mM, **B**) nitrate supply. (**C, D**) Root fresh weight of plants grown under limiting (0.5 mM, **C**) and non-limiting (5 mM, **D**) nitrate supply. (**E, F**) Shoot/root ratio of plants grown under limiting (0.5 mM, **E**) and non-limiting (5 mM, **F**) nitrate supply. Data were obtained from six plants from two independent experiments. Significant differences between genotypes for each nitrate supply condition were determined by Student's t-test (* *P*-value ≤ 0.05). **(G, H)** Top view of rosettes of Col-0 and *nup98anup98b*-double mutants grown under limiting (0.5 mM, **G**) and non-limiting (5 mM, **H**) nitrate supply at different times of the culture. Scale bar = 2 cm.

Figure 5. **Growth and gene expression in response to nitrate are strongly impacted by the simultaneous loss of function of Nucleoporin 98A/B and NLP7**

(A-C) Plants were grown on sand under short days with a light intensity of 150 µE for 39 d (A, B) Rosette fresh weight of plants grown under limiting (0.5 mM, A) and non-limiting (5 mM, B) nitrate supply. (C) Top view of rosettes of plants grown under non-limiting (5 mM), Scale bar = 2 cm. (D-F) Seedlings were grown on vertical agar plates supplied with 9 mM nitrate medium. Rosette (D) and root (E) fresh weight of 15-day-old seedlings. (F) Ratio of the fresh weight of rosettes to roots. Data were obtained from 4 pools of 6-8 seedlings per experiment from two independent experiments. Significant differences between genotypes for each nitrate supply condition were determined by Student's t-test (* P-value ≤ 0.05). (G-J) Gene expression analysis. Relative transcript levels of selected genes after nitrate addition to N-starved 14-day-old seedlings. Expression was measured by RT-qPCR and normalized as a percentage of the expression of a constitutive synthetic gene composed of TIP41 (At4g34270) and ACTIN2 (ACT2, At3g18780). (G-I) Data are means ± standard error (SE, n = 4) of one representative experiment out of 2. Significant differences between

genotypes for each nitrate supply condition were determined by Mann-Whitney. (J) Heatmap representation of the fold-change in steady state transcript level after 30 min of nitrate resupply in comparison to Col-0. Red, lower abundance; blue, higher abundance (* P-value ≤ 0.05 in comparison to nlp7-1).

Figure 6. **NUP98A *and* NUP98B loss of function abolished the nitrate-mediated nuclear accumulation of NLP7.**

Analysis of the nitrate-triggered nuclear accumulation of GFP-NLP7. **(A-H)** 10-days-old seedlings were N starved for 2 days before observation by confocal microscopy. Acquisitions were performed before nitrate addition **(A, C, E)**, or 10 min after nitrate addition **(B, D, F)**.

Representative images out of 3 independent experiments are shown. Scale bar = 50 µm.

(**G**) Nuclear-to-cytoplasmic fluorescence intensity ratios in plant cells across different samples. Ratios were calculated from measurements in 7-15 images per sample. Data are presented as boxplots. Statistical significance was assessed using the Kruskal–Wallis test followed by Dunn's post hoc test for pairwise comparisons. *P*-values: 1.49e-3 (**), 6.5e-6 (***). Black squares (■) and black downward triangles (▼): regular outliers; white upward triangle (△): extreme outlier.

Supplemental data

Supplemental Table S1. **Primers used for cloning, genotyping and RT-qPCR analyses.**

Supplemental Data Set 1. **NUP98A cDNA sequence optimized for *Arabidopsis thaliana,* synthetized and cloned into pTwist ENTR Kozak entry vector by Twist Biosciences**

Supplemental Figure S1. **NLP7 GAF and PB1 domains are not essential for the NLP7-NUP98A interaction**

NLP7ΔGAF and NLP7ΔPB1, interact with NUP98A in BiFC assays in *N. benthamiana* (**A-C**) NLP7-NUP98A interaction, (**D-F**) NLP7ΔGAF-NUP98A interaction, **(G-I)**

NLP7ΔPB1-NUP98A interaction. (**A, D, G**) YFP fluorescence (green), (**B, E, H**) chlorophyll autofluorescence (magenta), (**C, F, I**) YFP fluorescence (green) was merged with chlorophyll autofluorescence (magenta). Scale bar = 50 µm.

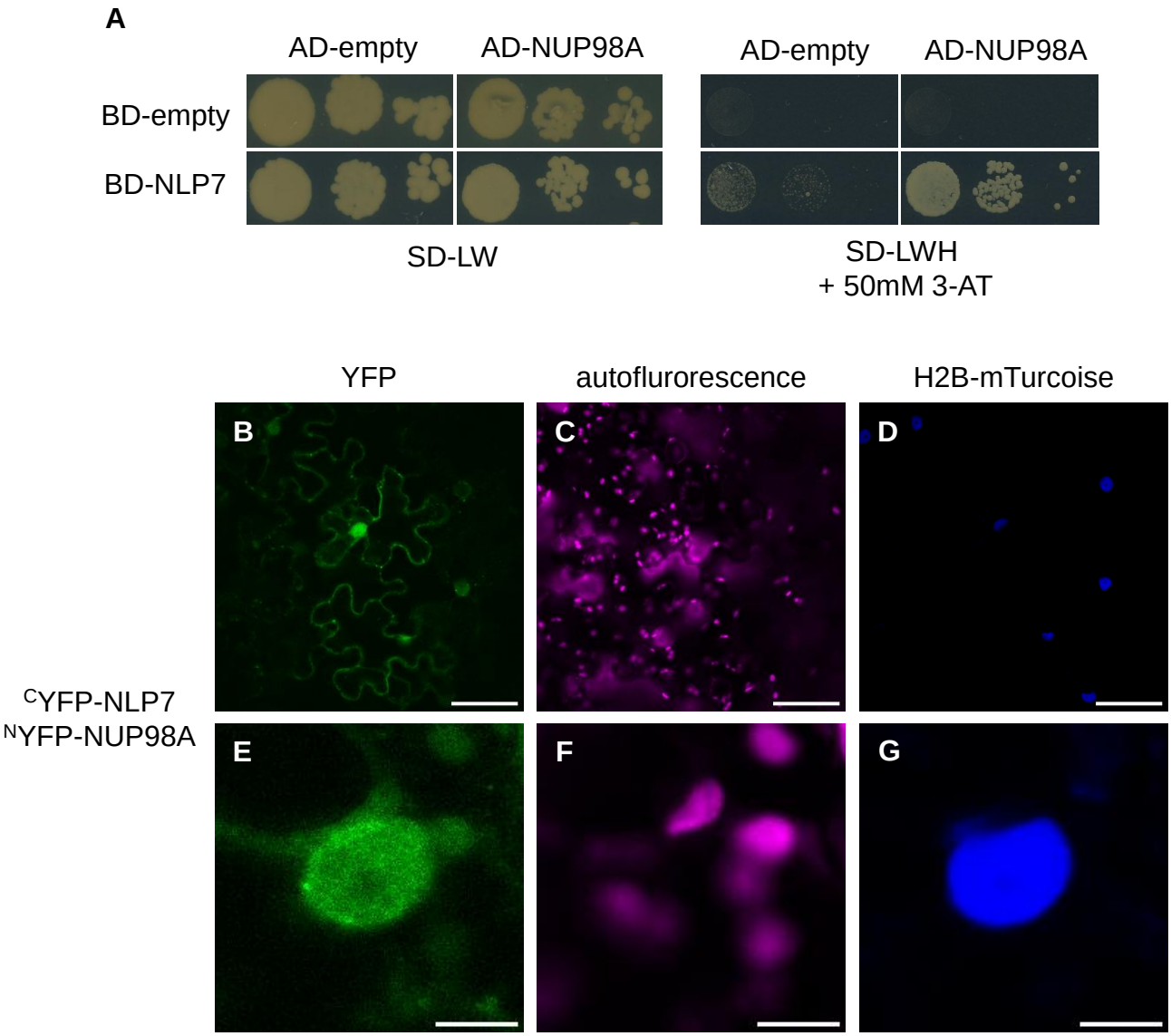

Figure 1. **NLP7 interacts with NUP98A.**

(**A**) Yeast two-hybrid assay using NLP7 fused with the binding domain (BD) and NUP98A fused with the DNA activation domain (AD). Cells were grown on selective and non-selective plates.

(**B-G**) NLP7 interacts with NUP98A in BiFC assays in *N. benthamiana.*

(**B, E**) YFP fluorescence (green), (**C, F**) chlorophyll autofluorescence (magenta), (**D, G**) H2B nuclear marker - mTurcoise fluorescence (blue)

Scale bar = (**B-D**) 50 µm, (**E-F**) 5 µm

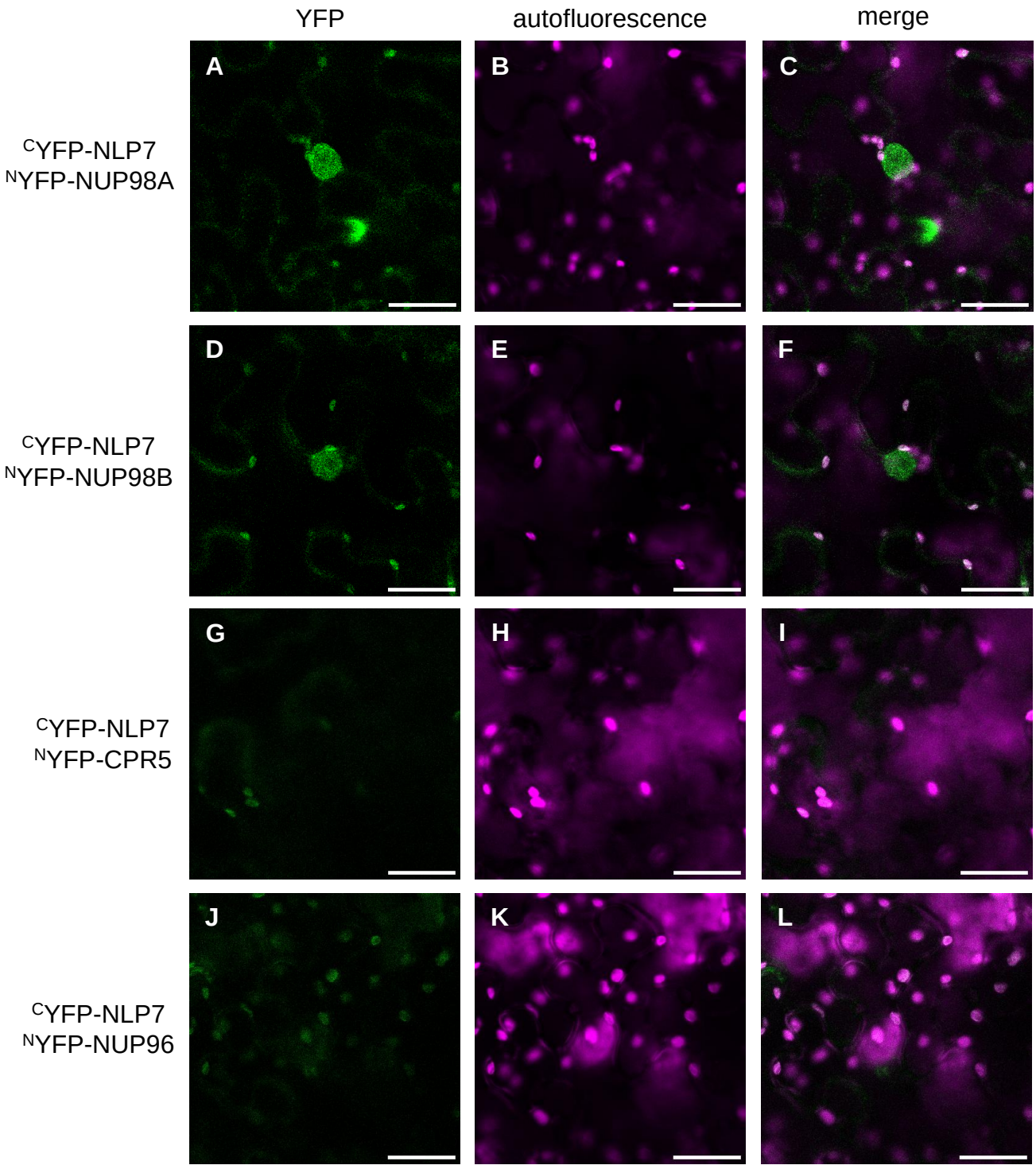

Figure 2. **NLP7 interacts with NUP98A and NUP98B.**

(A-L) NLP7 interacts with NUP98A and NUP98B in BiFC assays in *N. benthamiana.* (**A-C**) NLP7-NUP98A interaction, (**D-F**) NLP7-NUP98B interaction, **(G-I)** NLP7-CPR5 interaction (negative control), **(J-L)** NLP7-NUP96 interaction (negative control). (**A, D, G, J**) YFP fluorescence (green), (**B, E, H, K**) chlorophyll autofluorescence (magenta) (**C, F, I, L**) YFP fluorescence (green) was merged with chlorophyll autofluorescence (magenta)

Scale bar = 25 µm.

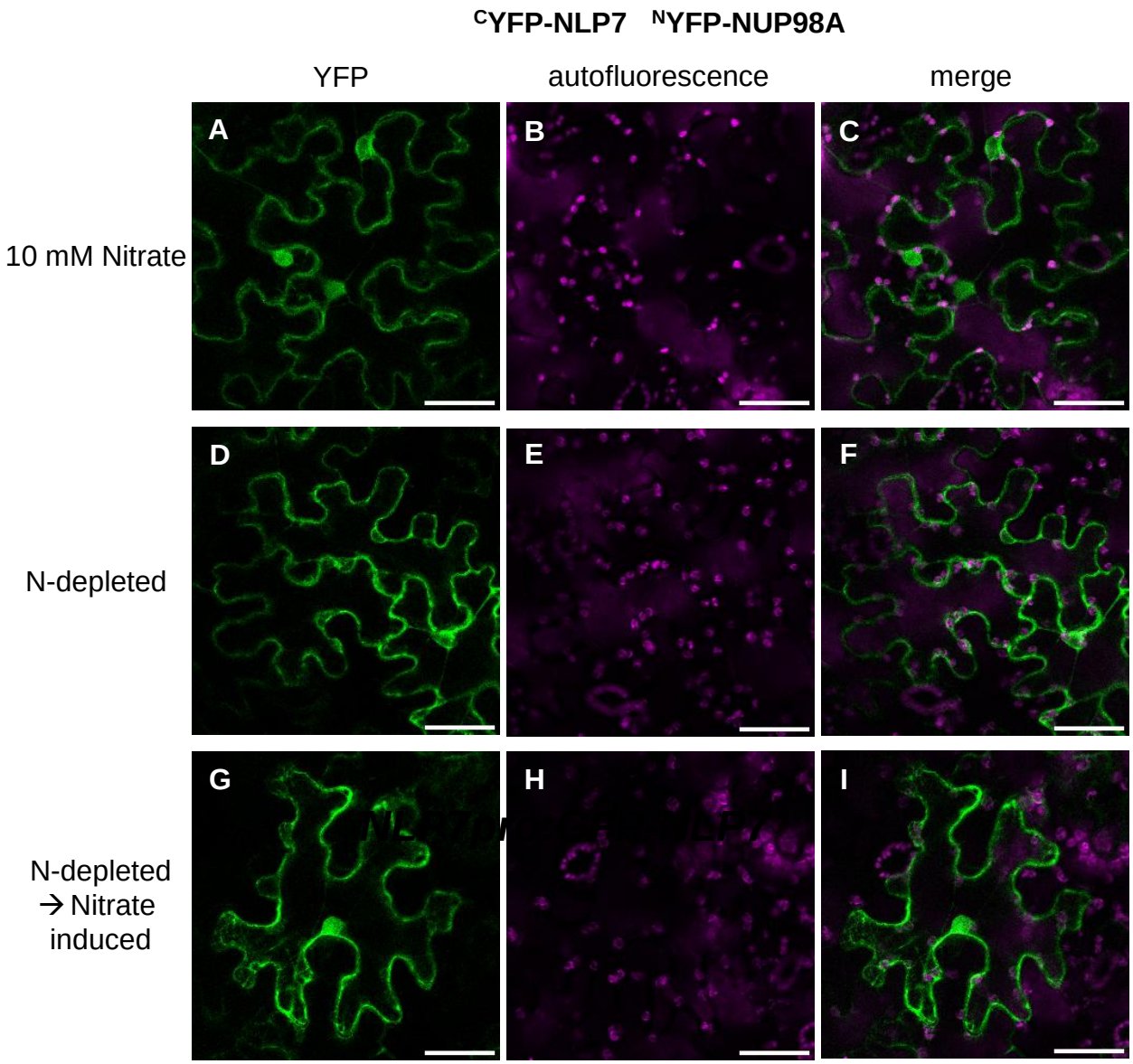

Figure 3. **NLP7 interacts with NUP98A in the nucleus in the presence of nitrate**

(A-I) BiFC assays between NLP7 and NUP98A in *N. benthaminia.* (**A-C**) Plants were supplied with 10 mM nitrate nutrition solution (**D-F**) Plants have been N-depleted for 5-days **(G-I)** leaf disc from transitory transformed N-depleted plants were treated for 10 min with nitrate. (A, D, G) YFP fluorescence (green), (B, E, H) chlorophyll autofluorescence (magenta) (C, F, I) YFP fluorescence (green) was merged with chlorophyll autofluorescence (magenta). Scale bar = 50 µm. **(J)** Nuclear-to-cytoplasmic fluorescence intensity ratios in plant cells across different samples. Ratios were calculated from measurements in 13-15 images per sample. Data are presented as boxplots. Statistical significance was assessed using the Kruskal–Wallis test followed by Dunn's post hoc test for pairwise comparisons. *P*-values: 4.47e-02 (**), 2.7e-07 (***), 1.08e-03 (###) .

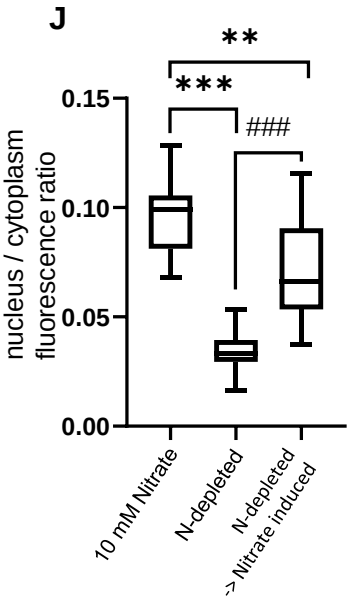

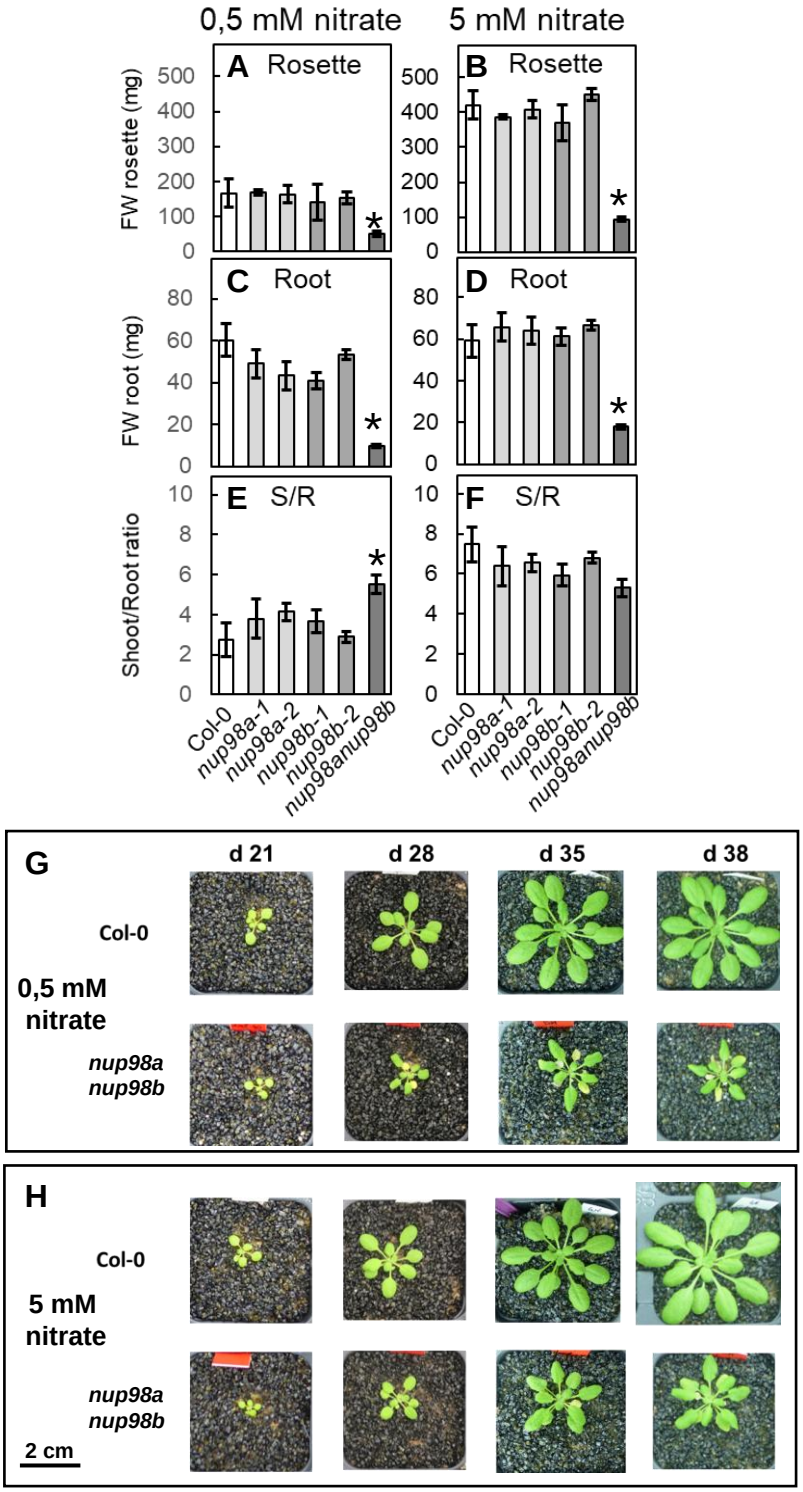

Figure 4. **Biomass and Shoot/Root ratio of *nup98a/b single and double* mutants grown under limiting and non-limiting nitrate supply.**

Plants were grown on sand under short days with a light intensity of 150 µE for 39 d (**A, B**) Rosette fresh weight of plants grown under limiting (0.5 mM, **A**) and non-limiting (5 mM, **B**) nitrate supply. (**C, D**) Root fresh weight of plants grown under limiting (0.5 mM, **C**) and non-limiting (5 mM, **D**) nitrate supply. (**E, F**) Shoot/root ratio of plants grown under limiting (0.5 mM, **E**) and non-limiting (5 mM, **F**) nitrate supply. Data were obtained from six plants from two independent experiments. Significant differences between genotypes for each nitrate supply condition were determined by Student t-Test (* *P*-value ≤ 0.05). **(G, H)** Top view of rosettes of Col-0 and *nup98anup98b*-double mutants grown under limiting (0.5 mM, **G**) and non-limiting (5 mM, **H**) nitrate supply at different times of the culture. Scale bar = 2 cm.

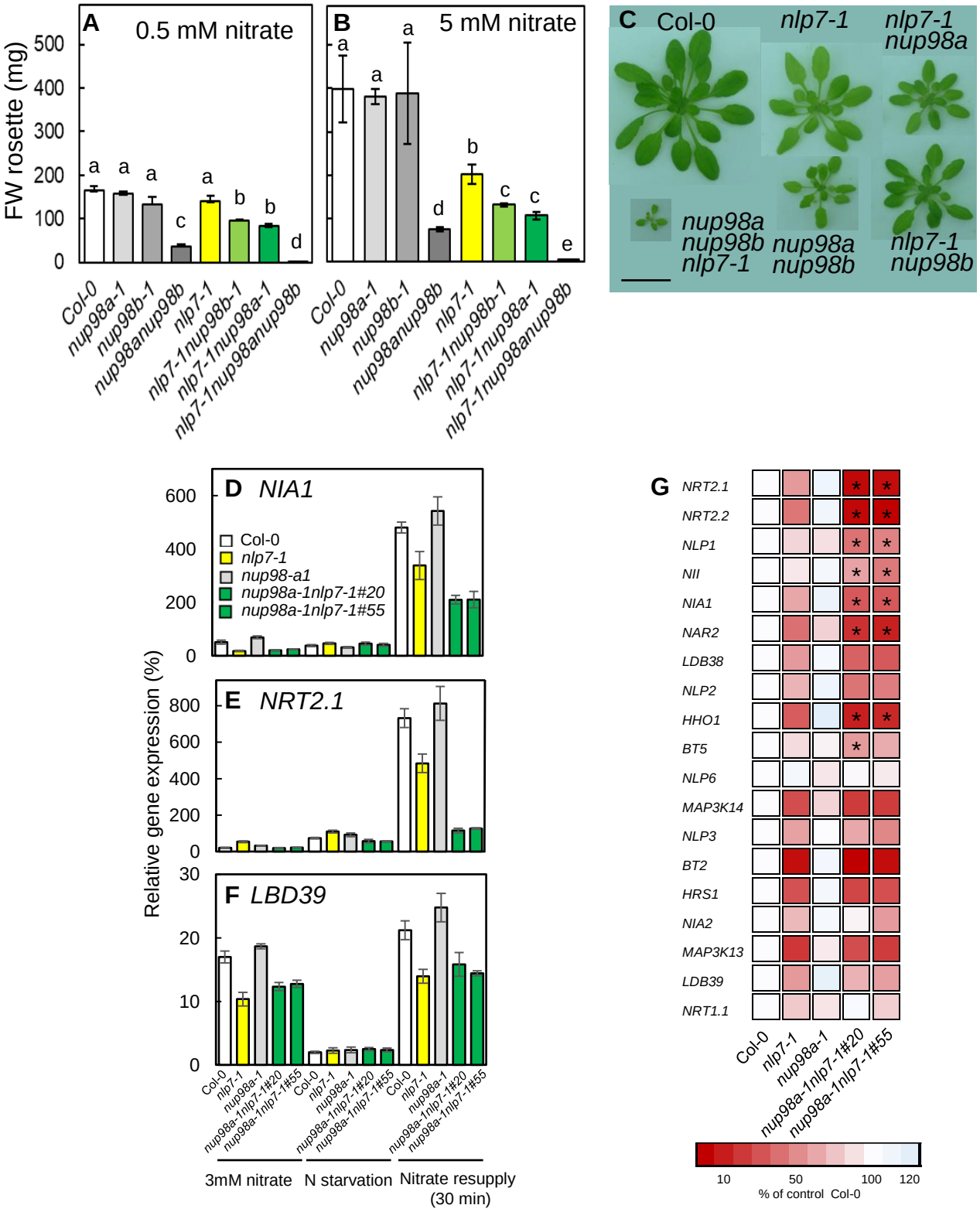

Figure 5. **Growth and gene expression in response to nitrate are strongly impacted by the simultaneous loss of function of Nucleoporin 98A/B and NLP7 (A-C)** Plants were grown on sand under short days with a light intensity of 150 µE for 39 d (**A, B**) Rosette fresh weight of plants grown under limiting (0.5 mM, **A**) and non-limiting (5 mM, **B**) nitrate supply. **(C)** Top view of rosettes of plants grown under non-limiting (5 mM), Scale bar = 2 cm. **(D-F)** Gene expression analysis. Relative transcript levels of selected genes before and after nitrate addition to N-starved 14-day-old seedlings. Expression was measured by RT-qPCR and normalized as a percentage of the expression of a constitutive synthetic gene composed of *TIP41* (At4g34270) and *ACTIN2* (*ACT2*, At3g18780). **(G)** Heatmap representation of the fold-change in steady state transcript level after 30 min of nitrate resupply in comparison to Col-0. Red, lower abundance; blue, higher abundance (* *P*-value ≤ 0.05 in comparison to *nlp7-1*).

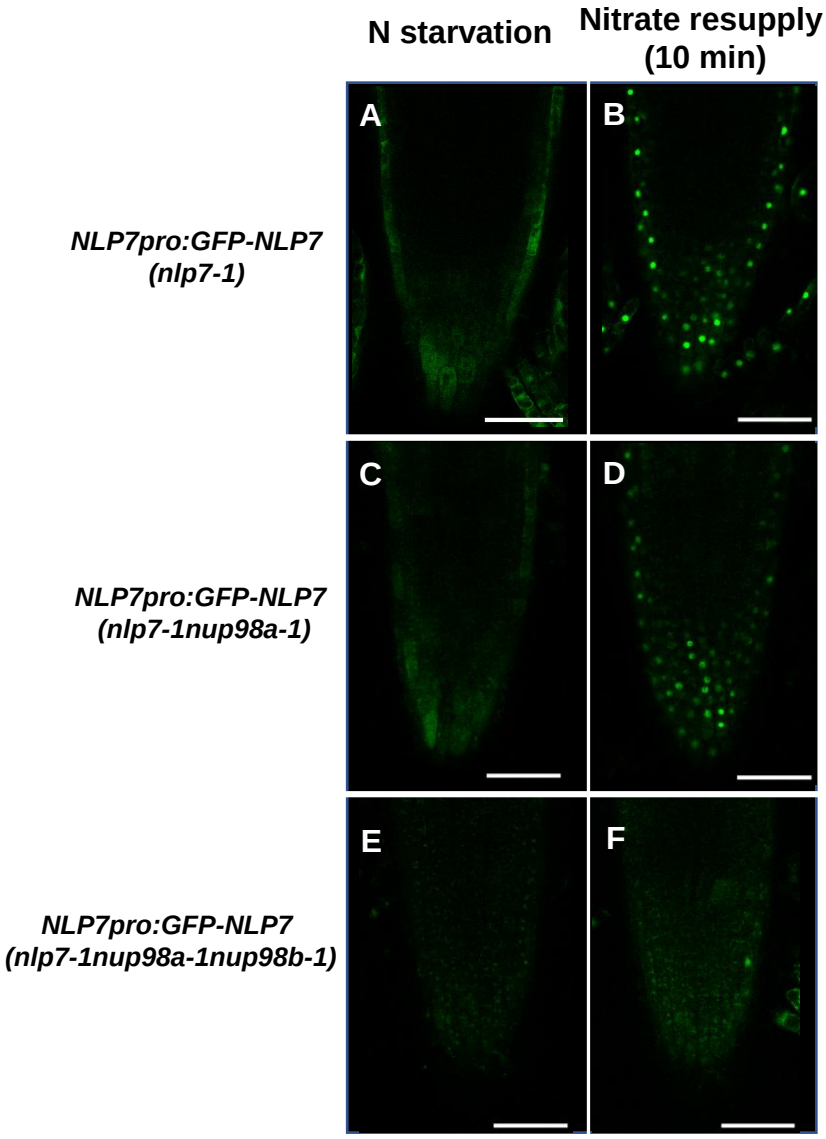

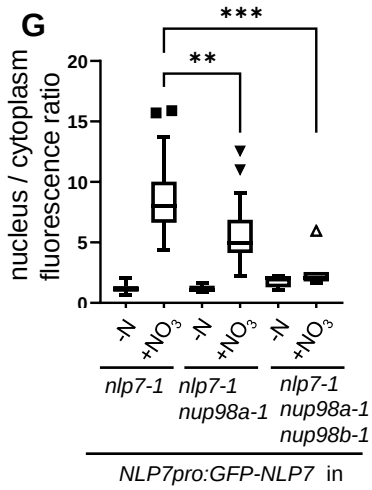

Figure 6. **NUP98A *and* NUP98B loss of function abolished the nitrate-mediated nuclear accumulation of NLP7.**

Analysis of the nitrate-triggered nuclear accumulation of GFP-NLP7. **(A-H)** 10-days-old seedlings were N starved for 2 days before observation by confocal microscopy. Acquisitions were performed before nitration addition **(A, C, E)**, or 10 min after nitrate addition **(B, D, F)**.

Representative images out of 3 independent experiments are shown. Scale bar = 50 µm.

(**G**) Nuclear-to-cytoplasmic fluorescence intensity ratios in plant cells across different samples. Ratios were calculated from measurements in 7-15 images per sample. Data are presented as boxplots. Statistical significance was assessed using the Kruskal–Wallis test followed by Dunn's post hoc test for pairwise comparisons. *P*-values: 1.49e-3 (**), 6.5e-6 (***). Black squares (■) and black downward triangles (▼): regular outliers; white upward triangle (△): extreme outlier.

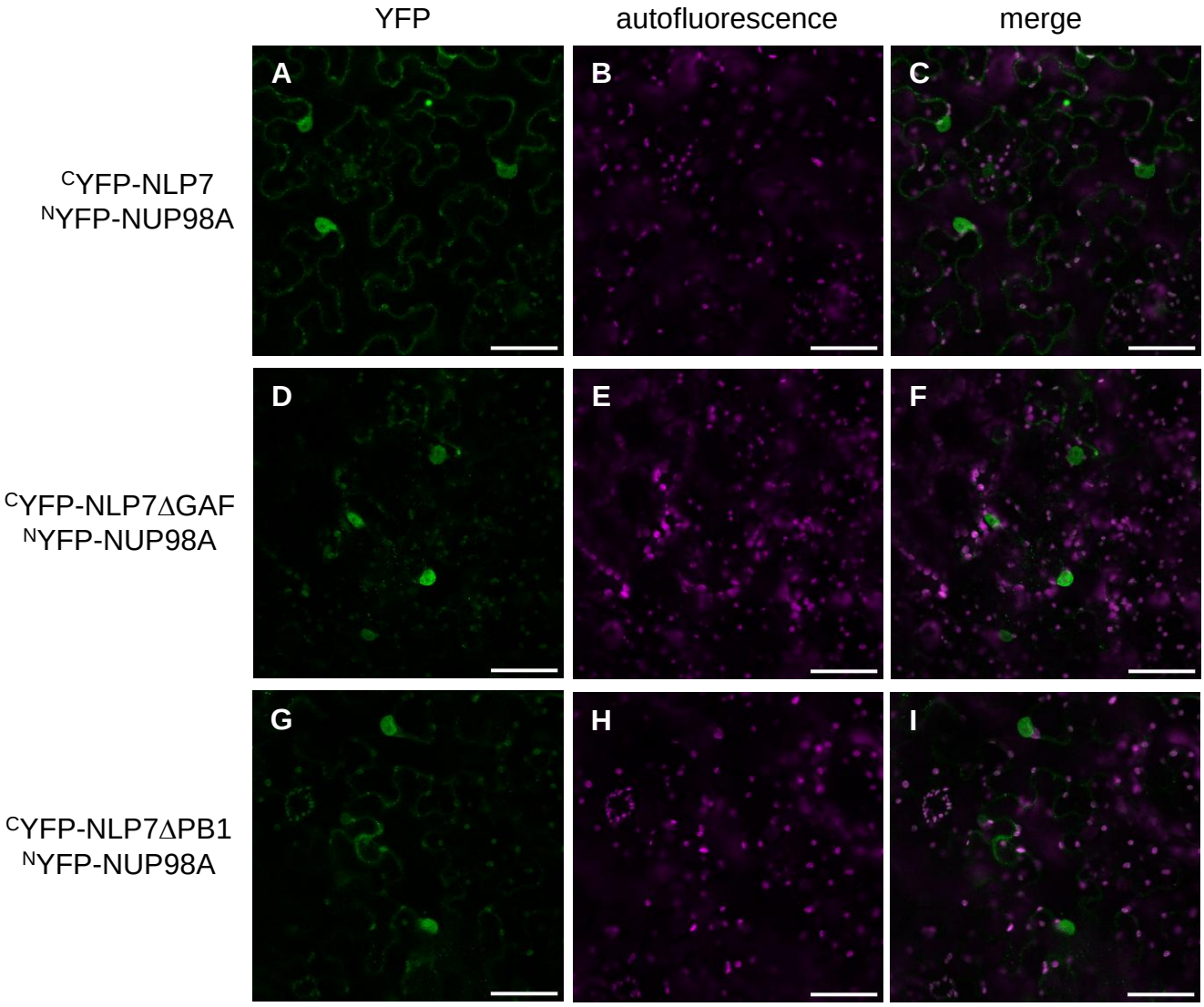

Supplemental Figure S1. **NLP7 GAF and PB1 domains are not essential for the NLP7-NUP98A interaction**

NLP7ΔGAF and NLP7ΔPB1, interact with NUP98A in BiFC assays in *N. benthamiana* (**A-C**) NLP7-NUP98A interaction, (**D-F**) NLP7ΔGAF-NUP98A interaction, **(G-I)** NLP7ΔPB1-NUP98A interaction. (**A, D, G**) YFP fluorescence (green), (**B, E, H**) chlorophyll autofluorescence (magenta) (**C, F, I**) YFP fluorescence (green) was merged with chlorophyll autofluorescence (magenta). Scale bar = 50 µm.